Supplementary Information

Impact of Defect dynamics on the formation of quantum emitters in hexagonal boron nitride

Pragya Joshi[1†], Sakal Singla[1†], Gabriel I. López Morales[2], Dushali Sharma[1], Surendra Kumar Makineni[3], Kenji Watanabe[4], Takashi Taniguchi[5], Suman Sarkar[6], Cyrus E. Dreyer[2,7*], Biswanath Chakraborty[1*]

[1]Department of Physics, Indian Institute of Technology Jammu, Jammu, 181221, Jammu and Kashmir, India.
[2]Department of Physics and Astronomy, Stony Brook University, Stony Brook, 11794, New York, USA.
[3]Department of Materials Engineering, Indian Institute of Science, Bengaluru, 560012, Karnataka, India.
[4]Research Center for Functional Materials, National Institute for Materials Science, 1-1 Namiki, Tsukuba, 305-0044, Japan.
[5]International Center for Materials Nanoarchitectonics, National Institute for Materials Science, 1-1 Namiki, Tsukuba, 305-0044, Japan.
[6]Department of Materials Engineering, Indian Institute of Technology Jammu, Jammu, 181221, Jammu and Kashmir, India.
[7]Center for Computational Quantum Physics,Flatiron Institute,162 5th Avenue, New York, New York 10010, USA.

*Corresponding author(s). E-mail(s): cyrus.dreyer@stonybrook.edu; biswanath.chakraborty@iitjammu.ac.in;
[†]These authors contributed equally to this work.

S1 - Raman Fitting Data for G peak

Raman peak fitting for the spectrums is shown in Figure 1d of the manuscript. Spectrum corresponding to sites S_a, S_b and S_c were fitted to obtain the carbon gradient graph shown in Figure 1e of the main manuscript.

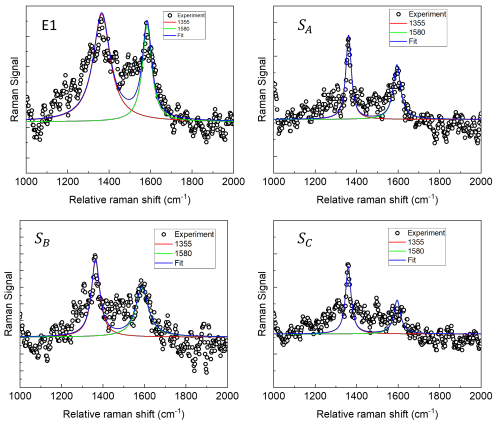

Fig. 1 Peak fitting for raman spectrum of site Epicenter E1 and site S_a, S_b, S_c.

S2 - Epicenter E2, E3, E4 analysis

Optical image in Fig 9a shows shows the location of all the epicenters. Encircled regions in Fig 9b are the sites where we observed PL signals. Raman signal captured from other E2, E3 and E4 (shown in Fig 9c) exhibit carbon features that are similar to those observed from epicenter E1 (figure 1d main text). We also observe a PL in the vicinity of each of the epicenters. Corresponding to epicenter E4 we see a broad PL peak at 2.05 eV a few microns away from site E4. Similarly, for epicenter E3 (E2), a PL peak at 2.15 eV (2.2 eV) is observed a few microns away from epicenter sites.

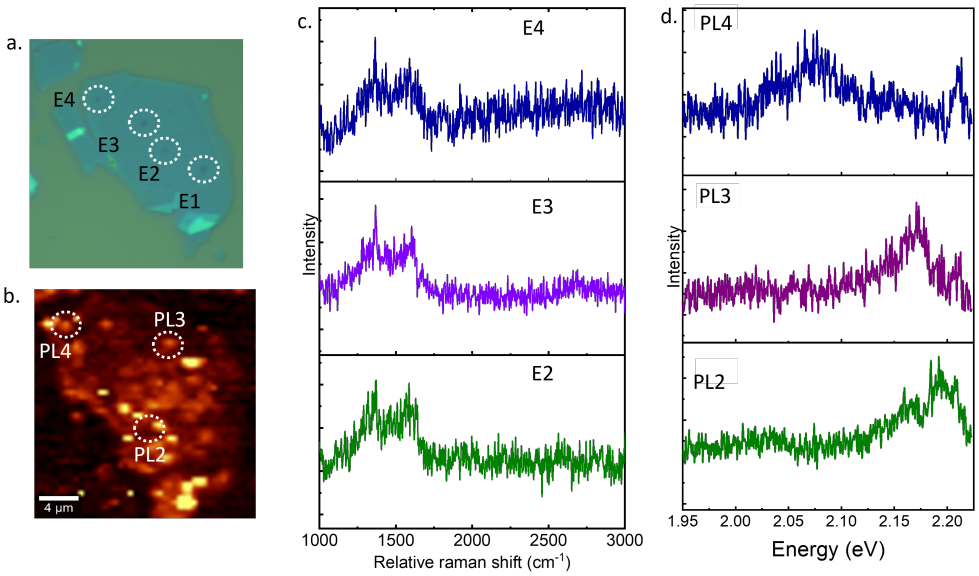

Fig. 2 Optical and PL image of flake with epicenter E1,E2,E3 and E4 highlighted by circles.Carbon raman signatures and PL corresponding to each epicenter is plotted.

S3 - SPE sample 2

Another sample with single photon emitter and migration trends as shown in the main manuscript.

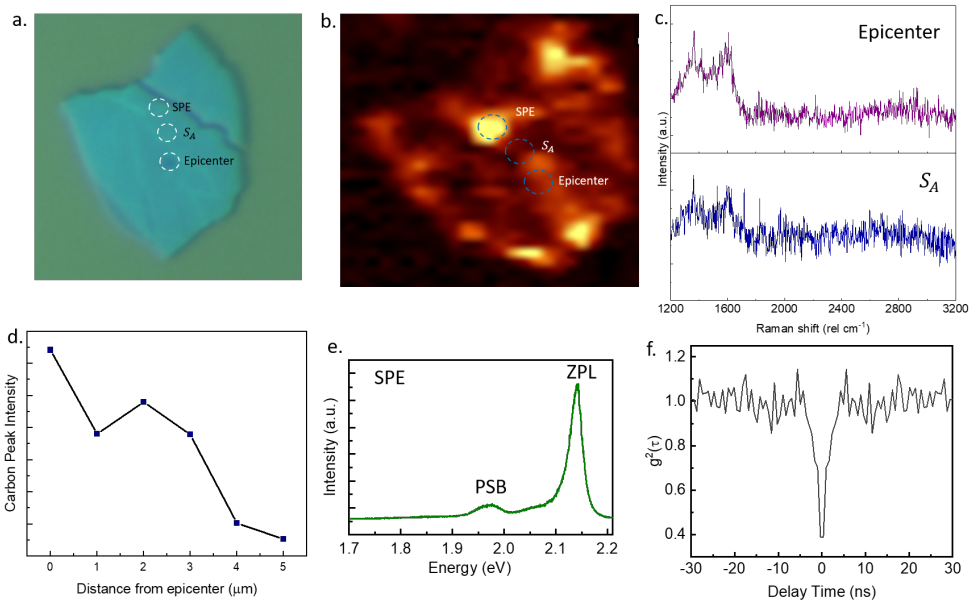

Fig. 3 a. Optical image showing Site 1 (Epicenter) , site 2 and site 3(SPE site). b. PL scan image of sample with encircled regions showing epicenter (red circle) and SPE site (blue circle). c. PL spectrum with ZPL and PSB. d. Antibunching dip of 0.39 obtained for the 578 nm signal. e. Raman spectrum from epicenter and site 2 showing gradual decay of carbon signatures. f. Carbon raman gradient as a function of distance from epicenter.

S4 - Location identification in TEM

After the flake was transferred on TEM grid , the location of interest was identified by mapping flake edges as shown in figure below.

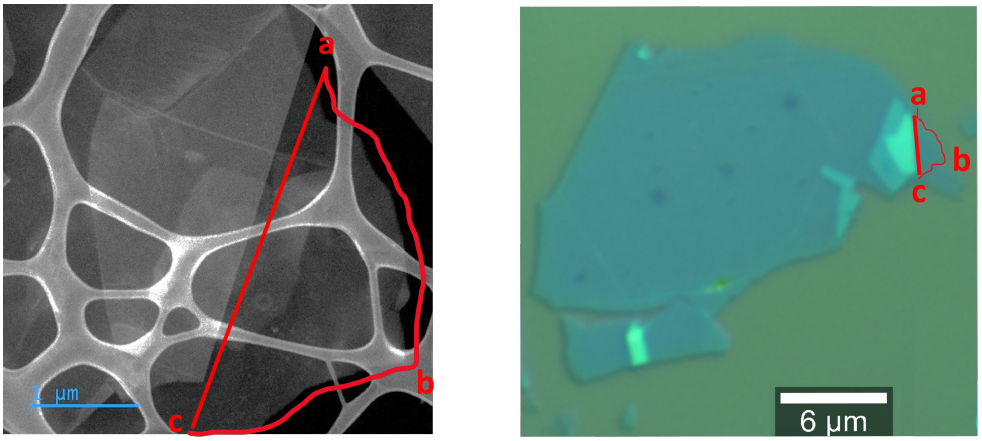

Fig. 4 Optical and HAADF image of the sample. Red dotted boundary used for identifying region of interest

S5 - EELS gradient mapping

Sequential EELS mapping of $S1, S_A, S_B, S_C, S_D, S_E$ and SPE site was performed. S1 and SPE maps are in the main manuscript while remaining data is shown below.

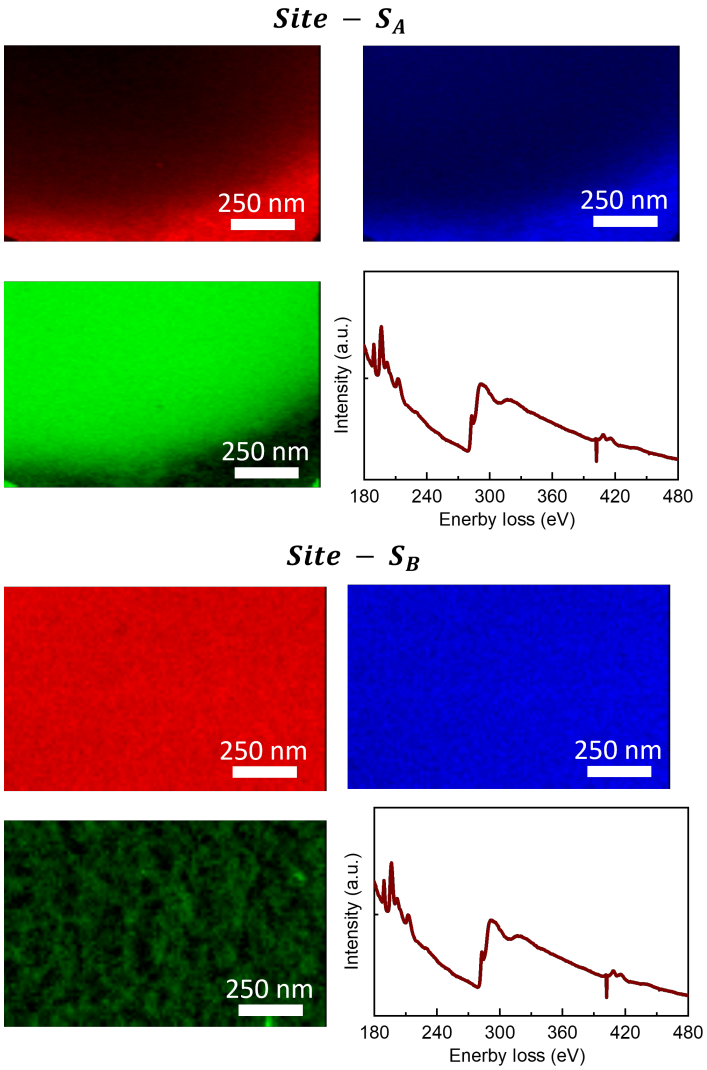

Fig. 5 EELS elemental maps and spectrum of site S_A and S_B showing boron (red), nitrogen(blue) and carbon (green) distribution.

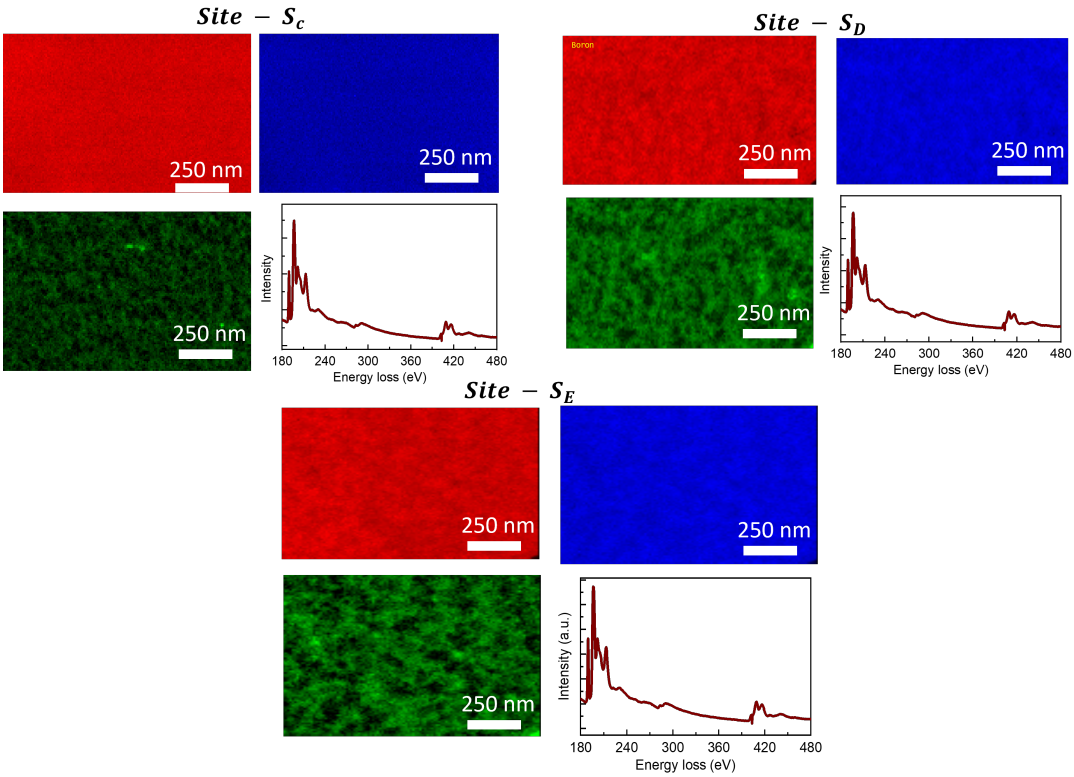

Fig. 6 EELS elemental maps and spectrum of site S_C , S_D and S_E showing boron (red), nitrogen(blue) and carbon (green) distribution.

S6 - High resolution image of SPE

Figure below shows magnified images captured from the SPE site. Multiple isolated small defect clusters exist inside the SPE region shown in figure 2i of the main manuscript. These individual sites lying on different layers of the sample could be acting as non interacting system. While the entire region is excited during PL measurement it is quite possible that only one of the encircled defect is optically active which gives rise to the antibunching peak observed in our experiments.

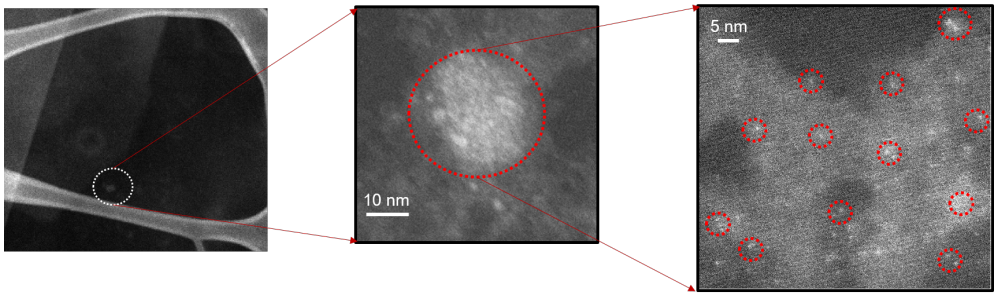

Fig. 7 High magnification image of the SPE carbon cluster showings smaller isolated defects (encircled in red).

S7 - Epicenter (Electron beam irradiated only)

For calculating the size of epicenter before annealing was fabricated using parameters similar to those described in the main manuscript. It can be observed that there is formation of carbon cluster just after the electron beam exposer. HAADF-STEM image of epicenter and their elemental analysis is shown in following figure

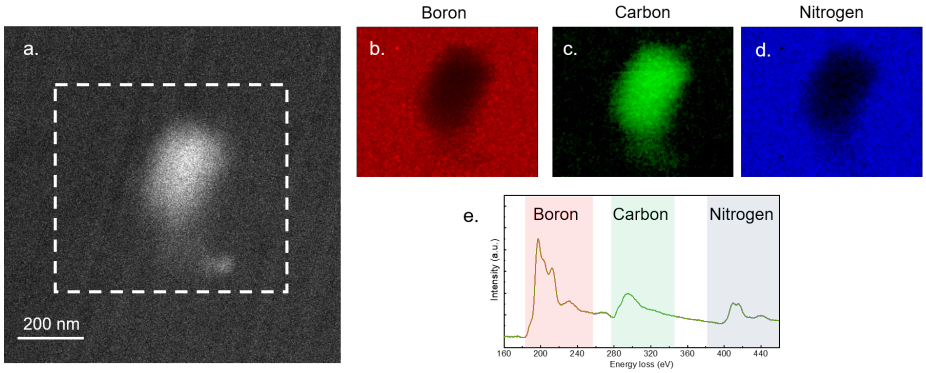

Fig. 8 (a) HAADF-STEm image of the epicenter before annealing (b-d) spatially resolved boron, carbon and nitrogen from the marked region (dotted square box) (e) Core energy loss spectrum from the same marked area.

S8 - Sample 3

The sample was fabricated using parameters similar to those stated in the main manuscript. Optical and PL image captured at each fabrication step are shown in the figure below. It can be seen that before annealing, there were no visible emitters in the h-BN flake. Analysis of the sample after annealing reveals multiple bright spots. The spectrum captured from the epicenter and emissive region shows a similar spectral trend as seen in the main manuscript. Carbonaceous raman signal from the epicenter (2k) and distinct emission peak at 564 nm from emissive site is observed.

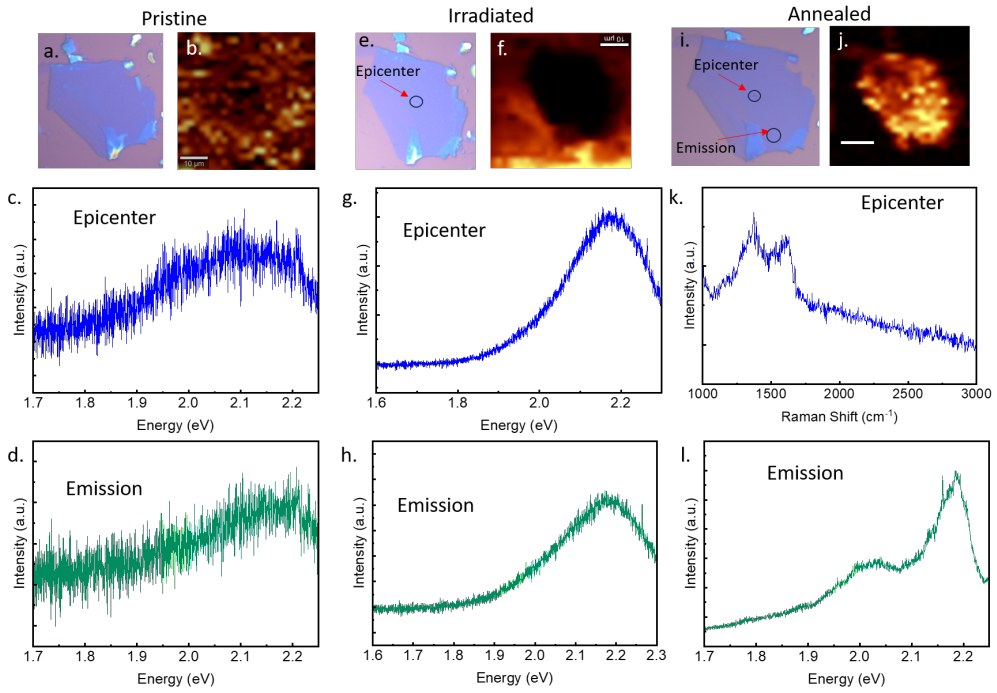

Fig. 9 Optical (a) and PL image (b) of pristine sample. c-d. Spectrum from different regions of pristine flake.Optical (e) and PL image (f) of the irradiated sample. The irradiation site 'epicenter' is highlighted by a black circle in the optical image. The spectrum obtained from the epicenter (g) and away area has similar spectral trends with a slight change in intensity. Optical (i) and PL (j) images of the annealed sample. The flake shows multiple bright regions in the PL image. The spectrum obtained from the epicenter (k) has a carbon signal similar to the main sample, while a few microns away, a distinct emission peak at 567 nm is observed.

S9 - Interplanar spacing analysis

Histogram plots showing the variation of interplanar spacing in the epicenter and emissive region. The top and bottom parts of both(epicenter and emissive) regions have been mapped out.

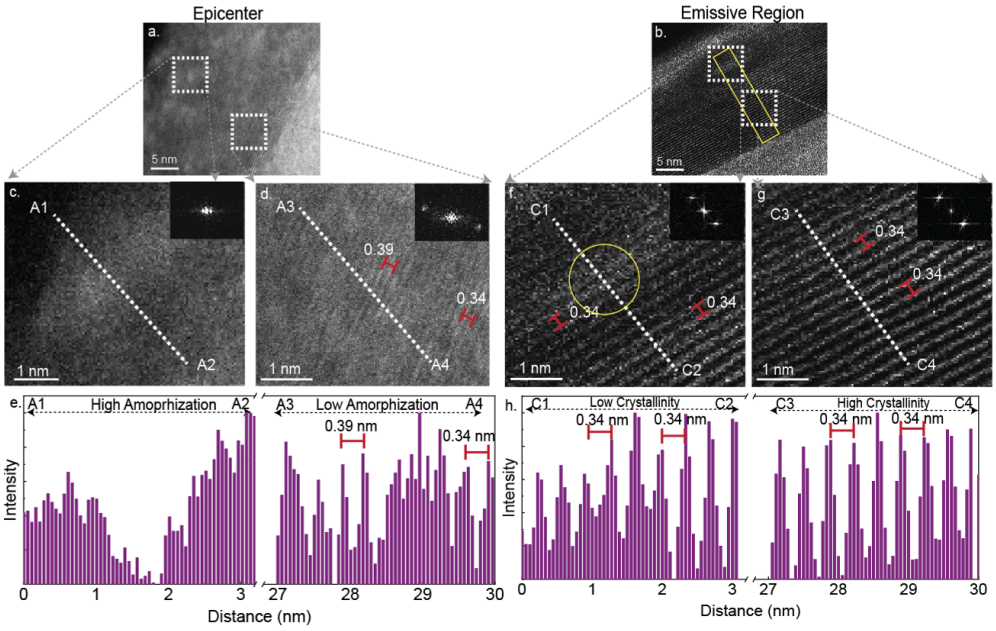

Fig. 10 a. Cross-sectional HAADF image of the epicenter region. b. Cross-sectional HAADF image of the emissive region. c,d. Magnified view of the top and bottom layers of the sample, respectively.e. Line profile analysis along A1-A2 and A3-A4 used for analysing interplanar distance. f,g. Top and bottom regions of emissive area reflecting perfectly ordered crystal planes with interplanar spacing 0.34 nm. Inset is the fast fourier transformed (FFT) image supporting crystalline behaviours. h. Line profile analysis used for calculating interplanar distance.